



HAL
open science

Adsorption of textile dyes on raw and decanted Moroccan clays: Kinetics, equilibrium and thermodynamics

R. Elmoubarki, F.Z. Mahjoubi, H. Tounsadi, J. Moustadraf, M. Abdennouri, T. Zouhri, Abderrazak El Albani, N. Barka

► **To cite this version:**

R. Elmoubarki, F.Z. Mahjoubi, H. Tounsadi, J. Moustadraf, M. Abdennouri, et al.. Adsorption of textile dyes on raw and decanted Moroccan clays: Kinetics, equilibrium and thermodynamics. WATER RESOURCES AND INDUSTRY, 2015, 9, pp.16-29. 10.1016/j.wri.2014.11.001 . hal-01334920

HAL Id: hal-01334920

<https://hal.science/hal-01334920>

Submitted on 15 Sep 2021

HAL is a multi-disciplinary open access archive for the deposit and dissemination of scientific research documents, whether they are published or not. The documents may come from teaching and research institutions in France or abroad, or from public or private research centers.

L'archive ouverte pluridisciplinaire **HAL**, est destinée au dépôt et à la diffusion de documents scientifiques de niveau recherche, publiés ou non, émanant des établissements d'enseignement et de recherche français ou étrangers, des laboratoires publics ou privés.



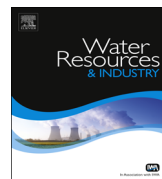
Distributed under a Creative Commons Attribution 4.0 International License



Contents lists available at ScienceDirect

Water Resources and Industry

journal homepage: www.elsevier.com/locate/wri



Adsorption of textile dyes on raw and decanted Moroccan clays: Kinetics, equilibrium and thermodynamics

R. Elmoubarki^{a,b}, F.Z. Mahjoubi^a, H. Tounsadi^a, J. Moustadraf^a,
M. Abdennouri^a, A. Zouhri^b, A. El Albani^c, N. Barka^{a,*}

^a Univ Hassan 1, Laboratoire des Sciences des Matériaux, des Milieux et de la Modélisation (LS3M), BP.145, 25000 Khouribga, Morocco

^b Univ Hassan 1, Laboratoire Chimie Appliquée et Environnement, 26000 Settat, Morocco

^c Université de Poitiers UFR SFA, UMR 6269 (HydrASA) Bat. Sciences Naturelles 40, Av. du Recteur Pineau, 86022 Poitiers Cedex, France

ARTICLE INFO

Article history:

Received 13 August 2014

Received in revised form

28 September 2014

Accepted 3 November 2014

Keywords:

Clays

Adsorption

Textile dyes

Equilibrium

Thermodynamics

ABSTRACT

Inexpensive and easily available Moroccan natural clays were investigated for the removal availability of textile dyes from aqueous solution. For this purpose, the adsorption of methylene blue (MB) as reference molecule, malachite green (MG) representative of cationic dyes and methyl orange (MO) representative of anionic dyes, was studied in batch mode under various parameters. The clays were characterized by means of XRD, cationic exchange capacity and BET surface area analysis. The experimental results show that, the adsorption was pH dependent with a high adsorption capacity of MB and MG in basic range and high adsorption of MO in acidic range. The pseudo-second-order kinetic model provided the best fit to the experimental data for the adsorption of MB and MG by the clays. However, the adsorption of MO was more suitable to be controlled by an intra-particle diffusion mechanism. The equilibrium adsorption data were analyzed by Langmuir, Freundlich and Dubinin–Radushkevich isotherm models. The adsorption process was found to be exothermic in nature in the case of MB and MO. However, the adsorption of MG was endothermic.

© 2014 The Authors. Published by Elsevier B.V. This is an open access article under the CC BY license (<http://creativecommons.org/licenses/by/3.0/>).

* Corresponding author. Tel.: +212 661 66 66 22; fax: +212 523 49 03 54.

E-mail address: barkanouredine@yahoo.fr (N. Barka).

1. Introduction

Organic dyes constitute one of the larger groups of pollutants in wastewater released from textile and other industries. Among 7×10^5 t and approximately 10,000 different types of dyes and pigments produced world wide annually, it is estimated that 1–15% of the dye is lost in the effluents during the dyeing process [1]. This massive influx of untreated organic chemicals into the waterways not only introduces aesthetic concerns, but far more importantly it promotes eutrophication and adversely affects the environmental health of the region. It also represents an increasing environmental danger due to their refractory carcinogenic nature [2]. From an environmental point of view, the removal of synthetic dyes is of great concern. Among several chemical and physical methods, adsorption process is one of the effective techniques that have been successfully employed for color removal from wastewater.

Many adsorbents have been tested to reduce dye concentrations from aqueous solutions. Activated carbon is regarded as an effective but expensive adsorbent due to its high costs of manufacturing and regeneration [3]. In addition to activated carbon, some adsorbents including agricultural wastes [4,5], lignite [6], natural phosphate [7], chitosan [8], silica [9], kaolinite [10], hydroxyapatite [11,12], perlite [13], sepiolite [14], montmorillonite [15] and some natural biosorbents have also been reported [16,17]. However, studies in this field have not produced materials which meet all demands of adsorption activity. The use of natural materials is a promising alternative due to their relative abundance and their low commercial value.

Clays have a high adsorption capacity due to their lamellar structure which provides high specific surface areas [18], which may even exceed that of activated carbon under the same conditions of temperature and pH [19]. Adsorption and desorption of organic molecules in the clays are primarily controlled by surface properties of the clay and the chemical properties of the molecules [20].

The focus of the present study was to assess the potentiality of Moroccan natural clays as a low-cost adsorbent for the removal of methylene blue, malachite green and methyl orange from aqueous solution as an ideal alternative to the current expensive methods of removing dyes from wastewater.

Adsorption studies were carried out under various parameters such as pH, contact time, initial dye concentration and temperature. The adsorption kinetic data was tested by pseudo-first-order, pseudo-second-order and intra-particle diffusion kinetic models. The equilibrium data were analyzed using Langmuir, Freundlich and Dubinin–Radushkevich isotherm models. The thermodynamics of the adsorption was also evaluated.

2. Experimental

2.1. Materials

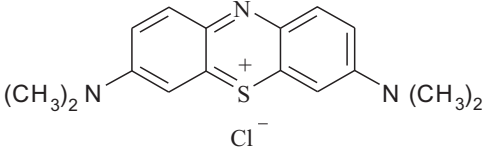
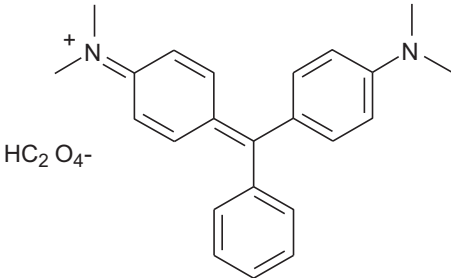
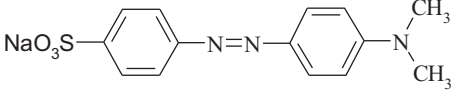
All the necessary chemicals used in the study were of analytical grade. Methylene bleu (MB), malachite green (MG) and methyl orange (MO) were provided by the Sigma-Aldrich chemicals and used without further purification. The chemical formula and some other specific characteristics of these dyes are summarized in Table 1.

2.2. Preparation and characterization of the adsorbents

The raw clays used in this work were collected from Safi and Berrechid regions in Morocco. The raw clays were purified according to the following procedure: clay dispersion was placed in a graduated cylinder for allowing particles $> 2 \mu\text{m}$ in size to settle down and the fine fraction, whose size was $< 2 \mu\text{m}$ was extracted at the time of the static sedimentation of the particles in suspension based on Stokes equation [21]:

$$t = 191.5 \times \frac{X}{d^2} \quad (1)$$

Table 1
Physicochemical characteristics of used dyes.

Name	Molecular structure	Nature	M_w (g/mol)	λ_{max} (nm)
Methylene blue (Basic blue 9)		Cationic	319.85	661
Malachite green (Basic green 4)		Cationic	329.5	621
Methyl orange (Acid orange 52)		Anionic	327.33	461

where: “ t ” is the necessary time (min), for a particle of diameter “ d ” (μm), to reach a depth of X (centimeter).

The solid samples were then dried at 105 °C for 24 h and then sieved in particles sizes lower than 100 μm . The obtained adsorbents were called; Safi raw clay (SRC), Safi decanted clay (SDC), Berrechid raw clay (BRC) and Berrechid decanted clay (BDC).

X-ray diffraction (XRD) patterns of the samples were obtained using a PANalytical Xpert Pro model diffractometer equipped with a monochromatic Cu- $K\alpha$ (1.541874 Å) source operating at 40 kV and 40 mA. The diffraction patterns were recorded between 5° and 65° (2θ) degrees. Specific surface area was determined by using N_2 as the sorbate at 77 K in a Micromeritics TriStar II 3020 sorptometer. Samples were out gassed prior to use at 473 K a night under vacuum. CEC of the materials was determined by extensive exchange with 1N ammonium acetate solution, followed by careful washing, drying and micro-Kjeldahl analysis by acid–base back-titration of the NH_3 desorbed from the NH_4^+ homoionized materials.

2.3. Adsorption tests

Stock solutions of 1 g/L of MB, MG and MO dyes were prepared by dissolving appropriate amount of each dye in distilled water and the used concentrations were obtained by dilution. Adsorption experiments were conducted in conical flasks at a constant agitation speed of 500 rpm by varying the pH of solution from 2 to 12, the adsorbent dosage from 0.5 to 10 g/L, the contact time from 5 to 300 min, the initial dyes concentrations from 50 to 250 mg/L and the temperature from 10 to 50 °C. The pH was adjusted to a given value by addition of HCl (1 N) or NaOH (1 N) and was measured using an EZODO pH-Meter. The temperature was controlled with using a thermostatically controlled incubator.

After each adsorption experiment completed, the sample were centrifuged at 3000 rpm for 10 min to separate the solid phase from the liquid phase. The supernatants were analyzed for residual dye concentrations by a Tomos V-1100 UV/Vis spectrophotometer.

The adsorbed quantity was calculated using the following equations:

$$q = \frac{(C_0 - C)}{R} \quad (2)$$

where q (mg/g) is the quantity of dye adsorbed per unit mass of adsorbent, C_0 (mg/L) is the initial dye concentration, C (mg/L) is the dye concentration after adsorption and R (g/L) is the mass of adsorbent per liter of aqueous solution.

2.4. Equilibrium isotherm modelling

Several theories of adsorption equilibrium were applied for the analysis of equilibrium sorption data obtained.

2.4.1. Langmuir model

The Langmuir adsorption model [22] is established on the following hypotheses: (1) uniformly energetic adsorption sites, (2) monolayer coverage, and (3) no lateral interaction between adsorbed molecules. Graphically, a plateau characterizes the Langmuir isotherm. Therefore, at equilibrium, a saturation point is reached where no further adsorption can occur. A basic assumption is that sorption takes place at specific homogeneous sites within the adsorbent. Once a dye molecule occupies a site, no further adsorption can take place at that site. A mathematical expression of the Langmuir isotherm is given by the following equation:

$$q_e = \frac{q_m K_L C_e}{1 + K_L C_e} \quad (3)$$

where q_e (mg/g) is the adsorbed amount at equilibrium, C_e is the equilibrium dye concentration (mg/L), K_L is Langmuir equilibrium constant (L/mg) and q_m the maximum adsorption capacity (mg/g).

2.4.2. Freundlich model

The Freundlich isotherm endorses the heterogeneity of the surface and assumes that the adsorption occurs at sites with different energy of adsorption. The energy of adsorption varies as a function of surface coverage [23]. This equation is also applicable to multilayer adsorption and is expressed by the following equation:

$$q_e = K_F C_e^{1/n} \quad (4)$$

where K_F is the Freundlich constant and n is the heterogeneity factor. The K_F value is related to the adsorption capacity; while $1/n$ value is related to the adsorption intensity.

2.4.3. Dubinin–Radushkevich model

The Dubinin–Radushkevich isotherm model does not assumes a homogenous surface or constant sorption potential as other models. It can be noted that the (D–R) isotherm is more general than the Langmuir fit. The D–R isotherm has been written by the following equations [24]:

$$q_e = q_m \exp(-B\varepsilon^2) \quad (5)$$

$$\varepsilon^2 = RT \ln \left(1 + \frac{1}{C_e} \right) \quad (6)$$

where B is a constant related to the adsorption energy, q_m is the theoretical saturation capacity, ε is the Polanyi potential.

3. Results and discussion

3.1. Characterization of the clays

The constituent phases of the clay minerals, as well as the structural changes stemming from the decantation were evaluated by XRD analysis. The results are presented in Fig. 1a–d. Fig. 1a indicates that Berrechid raw clay (BRC) is mainly composed of quartz, clay, dolomite, hematite and feldspars. These latest are mainly represented by plagioclase associated with small quantities of potassium feldspar. After decantation (BDC), the suspended fraction is relatively impoverished of quartz and feldspars but enriched in clay (Fig. 1b). For the clay of Safi, the raw material (SRC) presented in Fig. 1c appears to have a clay/quartz ratio close to that of Berrechid. However, the carbonate content is much lower; moreover it consists on a combination of calcite and dolomite. Furthered, the hematite and feldspars are less abundant.

The predominant clay mineral of Berrechid raw clay (BRC) is illite associated with very small amounts of chlorite. These reports are not substantially modified after decantation (BDC). The Safi raw clay (SRC) is composed by a mixture of illite and kaolinite associated with small amounts of chlorite. Like the clay of Berrechid, the collected clay after decantation (SDC) differs little from that analyzed directly on the raw clays (Fig. 1d).

The specific surface areas and cationic exchange capacities of the four samples are presented in Table 2. The analysis of the CEC indicates that Safi raw clay has a CEC ten times higher than that of Berrechid raw clay. In natural samples, the phases having the largest CEC are usually clays and iron oxides. However, at Berrechid, these latest are present as relatively well crystallized hematite form which has a low exchange capacity. Contrariwise, the largest proportion of clays in SRC is probably the cause of the high CEC. After decantation, the materials contain almost as clay minerals whose CEC is relatively low; illite, chlorite and kaolinite. This is why the CEC values are relatively close in the treated samples.

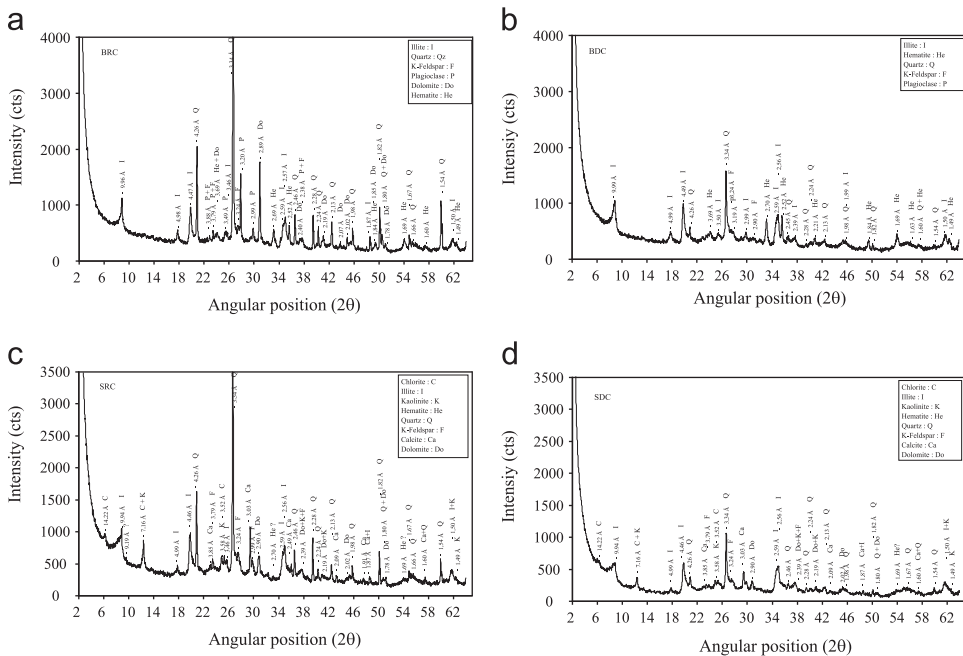


Fig. 1. (a) XRD patterns of Berrechid raw clay (BRC). (b) XRD patterns of Berrechid decanted clay (BDC). (c) XRD patterns of Safi raw clay (SRC). (d) XRD patterns of Safi decanted clay (SDC).

Table 2
Specific surface areas and cationic exchange capacities of the clays.

Clay	Surface area (m ² /g)	CEC (meq/100 g)
SRC	33.08	9.0
SDC	64.65	17.1
BRC	34.07	0.9
BDC	62.86	16.4

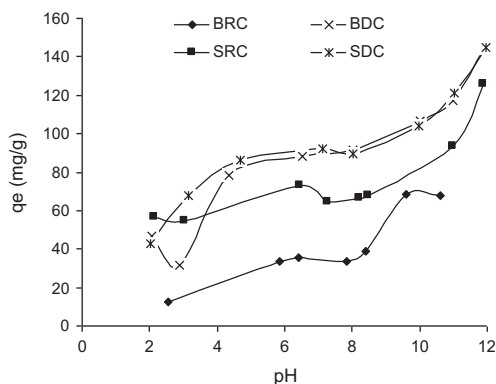


Fig. 2. Effect of pH on the adsorption of MB by the clays: $C_0=100$ mg/L, $R=0.5$ g/L, contact time=120 min, $T=25$ °C, Agitation=500 rpm.

The surface area of the decanted clays increased significantly from 33.08 m²/g to 64.65 m²/g for the clay of Safi and from 34.07 m²/g to 62.86 m²/g for the clay of Berrechid. The SDC has received maximum enhancement in surface area by 95%, followed by the BDC (84%). The increase in surface area resulted from the impoverishment of quartz and feldspars which have low surface areas compared to the clay phases.

3.2. Effect of pH on the adsorption of dyes

pH is the most important factors that influence adsorption process, because it can affect at the same time the surface charge of the adsorbent, the ionization degree of functional groups of the adsorbate, as well as the mechanism of adsorption. Changes observed in the adsorption of MB, MG and MO by raw and decanted clays are presented in Figs. 2–4. The figures indicate that, for methylene blue and malachite green, the adsorption is weak in acidic medium. As the pH increase, the adsorption capacity increases. For methyl orange, the adsorption is high in acidic medium and decreases with the increase in pH of the solution. According to this observation, two possible mechanisms of adsorption can be considered: electrostatic interactions between the surface groups of clays and the functional groups of dyes molecules, and or a chemical reaction between the clays and the dyes molecules. As long as the pH of the system decreased, the number of positively charged sites increased, and the number of negatively charged sites decreased. On the first hand negatively charged sites on the adsorbent surface favored the adsorption of cationic dye due to this interaction. On the other hand, the lower adsorption at acid pH was due to the presence of excess H⁺ competing with the cationic dye for adsorption sites. Lower sorption of the anionic dye at alkaline pH could be attributed to the abundance of OH⁻ ions which will compete with the dye anions for the same sorption sites [25]. This suggests that the first mechanism, electrostatic interactions, might be operative. Further adsorption experiments were conducted at initial solutions pH of 7.5 for MB and MG and 6.5 for MO.

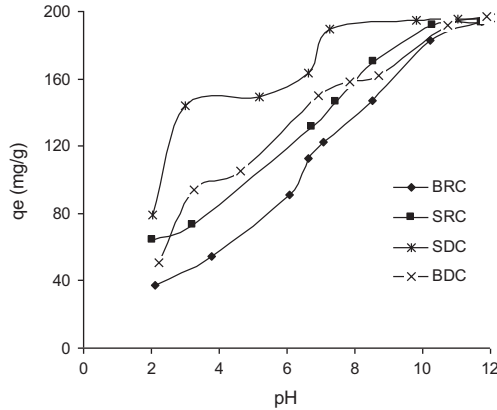


Fig. 3. Effect of pH on the adsorption of MG by the clays: $C_0=100$ mg/L, $R=0.5$ g/L, contact time=120 min, $T=25$ °C, Agitation=500 rpm.

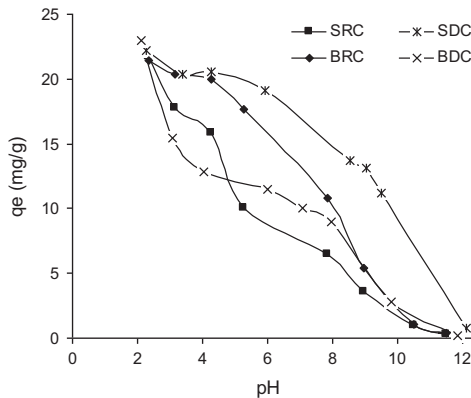


Fig. 4. Effect of pH on the adsorption of MO by the clays: $C_0=100$ mg/L, $R=4$ g/L, contact time=120 min, $T=25$ °C, Agitation=500 rpm.

3.3. Adsorption kinetics

The kinetics of the adsorption of methylene blue, malachite green and methyl orange by raw and decanted clays are presented in Figs. 5–7. The figures indicate that, the removal of cationic dyes (MB and MG) was very rapid in the first 5–10 min of contact time; around 90% of equilibrium yield was obtained in this period. After this period, the rate of removal be slower and stagnates with the increase in contact time. For methyl orange, the kinetics was found to be much slower.

In order to characterize the kinetics involved in the process of adsorption, pseudo-first-order and pseudo-second-order kinetic models were proposed and the kinetic data were analyzed based on the regression coefficient, (r^2), and the amount of dye adsorbed at equilibrium.

The pseudo-first-order rate expression of Lagergren based on solid capacity is generally expressed as follows [26]:

$$\frac{dq}{dt} = k_1(q_e - q) \quad (7)$$

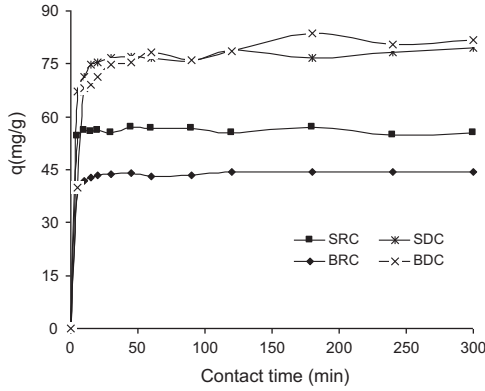


Fig. 5. Kinetics of the adsorption of MB by the clays: $C_0=100$ mg/L, $R=1$ g/L, $pH=7.5$, $T=25$ °C, Agitation=500 rpm.

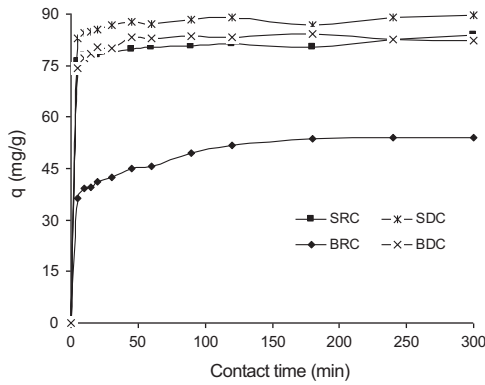


Fig. 6. Kinetics of the adsorption of MG by the clays: $C_0=100$ mg/L, $R=1$ g/L, $pH=7.5$, $T=25$ °C, Agitation=500 rpm.

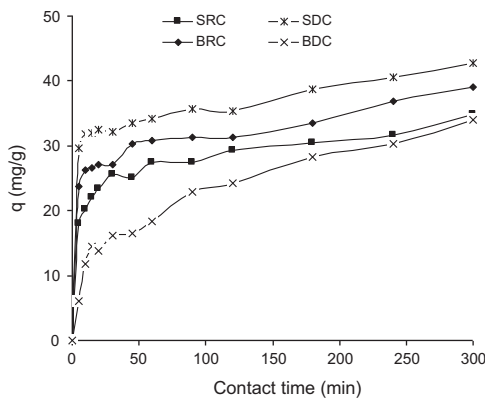


Fig. 7. Kinetics of the adsorption of MO by the clays: $C_0=100$ mg/L, $R=2$ g/L, $pH=6.5$, $T=25$ °C, Agitation=500 rpm.

After integrating and applying the boundary conditions, for $q=0$ at $t=0$ and $q=q$ at $t=t$, the integrated form of Eq. (7) becomes:

$$q = q_e \left(1 - e^{-k_1 t} \right) \tag{8}$$

Table 3
Kinetic constants for dyes adsorption onto clays.

Dye	Clay	Pseudo-first-order			Pseudo-second-order			Intra-particle diffusion model		
		q_e (mg/g)	k_1 (1/min)	r^2	q_e (mg/g)	k_2 (g/mg min)	r^2	k_{id} (mg/g min ^{0.5})	I (mg/g)	r^2
MB	SRC	56.05	0.700	0.998	56.25	0.130	0.998	0.076	55.71	0.135
	SDC	76.69	0.396	0.993	78.28	0.015	0.998	0.249	74.59	0.600
	BRC	43.71	0.444	0.997	44.38	0.036	0.999	0.095	42.90	0.660
	BDC	78.48	0.156	0.980	82.86	0.003	0.976	0.866	68.68	0.790
MG	SRC	80.17	0.591	0.993	81.22	0.029	0.997	0.423	76.27	0.909
	SDC	87.27	0.587	0.996	88.29	0.029	0.999	0.350	83.94	0.734
	BRC	48.22	0.200	0.886	51.43	0.006	0.955	1.228	35.76	0.932
	BDC	81.84	0.450	0.993	83.39	0.017	0.998	0.440	77.16	0.510
MO	SRC	27.78	0.139	0.919	29.86	0.007	0.975	0.814	19.99	0.954
	SDC	34.84	0.342	0.935	37.47	0.014	0.938	0.784	28.27	0.965
	BRC	31.71	0.206	0.861	33.88	0.009	0.927	0.857	23.25	0.950
	BDC	28.74	0.026	0.868	32.97	0.001	0.931	1.518	7.478	0.988

where q_e and q (both in mg/g) are respectively the amounts of dye adsorbed at equilibrium and at any time 't', and k_1 (1/min) is the rate constant of adsorption.

The pseudo-second-order model proposed by Ho and McKay [27] was used to explain the sorption kinetics. This model is based on the assumption that the adsorption follows second order chemisorption. The pseudo-second-order model can be expressed as:

$$\frac{dq}{dt} = k_2(q_e - q)^2 \quad (9)$$

After integrating for the similar boundary conditions, the following equation can be obtained:

$$q = \frac{k_2 q_e^2 t}{1 + k_2 q_e t} \quad (10)$$

where k_2 (g/mg min) is the rate constant of pseudo-second order adsorption.

For the interpretation of experimental kinetics data, from a mechanistic viewpoint, prediction of the rate-limiting step is an important consideration. The adsorbate transport from the solution phase to the surface of the adsorbent particles occurs in several steps. The overall adsorption process may be controlled either by one or more steps, e.g. film or external diffusion, pore diffusion, surface diffusion and adsorption on the pore surface, or a combination of more than one step. The possibility of intra-particle diffusion was explored by using the intra-particle diffusion model [28]:

$$q = k_{id} t^{0.5} + I \quad (11)$$

where k_{id} is the intra-particle diffusion rate constant (mg/g min^{1/2}) and I (mg/g) is a constant.

If the Weber–Morris plot of q versus $t^{0.5}$ satisfies the linear relationship with the experimental data, then the sorption process is found to be controlled by intra-particle diffusion only. However, if the data exhibit multi-linear plots, then two or more steps influence the sorption process.

Parameters of the pseudo-first-order and pseudo-second-order and intra-particle diffusion models were estimated with the aid of the non-linear regression. The obtained data and the correlation coefficients, r^2 , are given in Table 3. From these results, the pseudo-second order model seems to be more adapted to describe the adsorption dynamics of the cationic dyes (MB and MG) on the different clays due to the good correlation parameters calculated by the model with experimental data. However, the adsorption of anionic dye (MO) was more suitable to be controlled by an intra-particle diffusion mechanism. Since cationic dyes adsorption follows pseudo-second order kinetics, this suggested that boundary layer resistance was not the rate limiting step [29]. The rate of adsorption may be controlled largely by a chemisorption process, in conjunction with the chemical characteristics of the clays and dyes molecules.

3.4. Adsorption isotherms

The amounts of adsorbed quantities of each dye at the equilibrium (q_e), versus equilibrium dye concentration were drawn in Figs. 8–10. The experimental adsorption isotherms obtained were compared with the adsorption isotherm models and the constants appearing in each equation of those models were determined by nonlinear regression analysis. The results of this analysis are tabulated in Table 4. The square of the correlation coefficient (r^2) are also shown in this table.

The methylene blue and malachite green isotherms show an important adsorption with almost weak concentration in the solution, it is an isotherm of the type H in Giles classification [30]. Generally, Isotherms types H are the result of the dominance of strong ionic adsorbate–adsorbent interactions [31]. A chemical adsorption of positively charged functional groups of MB and MG on the negatively charged surface groups of the clays is proposed. The best fit of experimental data in the case of MB was obtained with the Langmuir model. This result suggests that the adsorption process of MB by the clays was monolayer adsorption, and the maximum monolayer adsorption capacities were found to be 75.18, 114.16, 49.01 and 95.50 mg/g, respectively, for SRC, SDC, BRC and BDC. For MG, the experimental result was good fitted with both Langmuir and Dubinin–Radushkevich isotherm models. The Langmuir adsorption capacities were found to be 156.43, 176.37, 86.55 and 109.82 mg/g, respectively, for SRC, SDC, BRC and BDC. This result showed that the malachite green is homogeneously adsorbed by means of ionic adsorption assured by the negatively charged surface of clays.

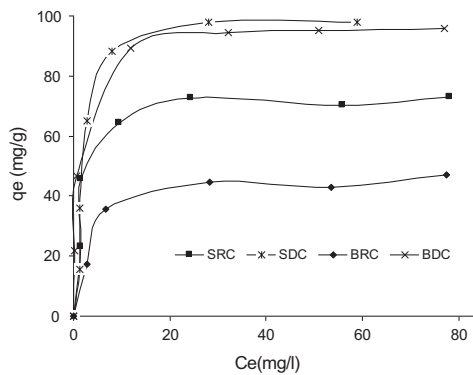


Fig. 8. Effect of MB concentration on its adsorption by the clays: $V=200$ mL, $R=1$ g/L, $\text{pH}=7.5$, $T=25$ °C, Agitation=500 rpm.

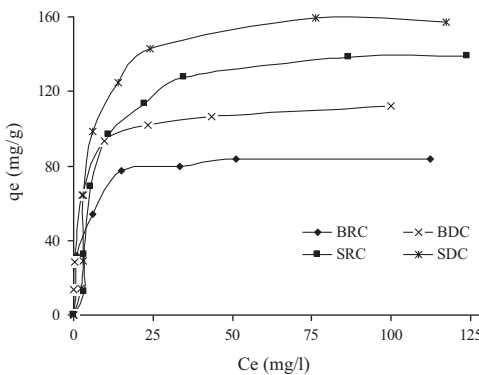


Fig. 9. Effect of MG concentration on its adsorption by the clays: $V=200$ mL, $R=1$ g/L, $\text{pH}=7.5$, $T=25$ °C, Agitation=500 rpm.

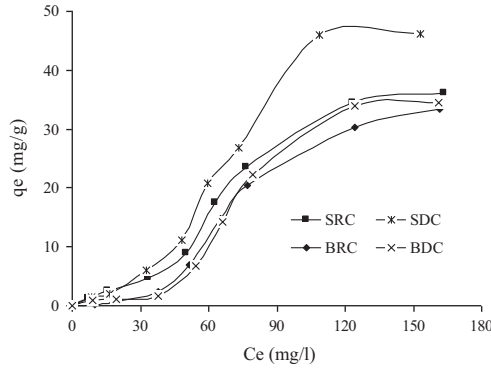


Fig. 10. Effect of MO concentration on its adsorption by the clays: $V=200$ mL, $R=1$ g/L, $\text{pH}=6.5$, $T=25$ °C, Agitation=500 rpm.

Table 4

Models isotherm constants for the dyes adsorption onto clays.

Dye	Clay	Langmuir			Freundlich			Dubinin–Radushkevich		
		q_m (mg/g)	K_L (L/mg)	r^2	K_F ($\text{mg}^{1-1/n}/\text{L}^{1/n}/\text{g}$)	n	r^2	q_m (mg/g)	B (mol/J)	r^2
MB	SRC	75.18	0.561	0.945	37.03	5.83	0.893	74.68	0.00062	0.867
	SDC	114.16	0.359	0.942	39.75	4.00	0.836	106.85	0.00087	0.930
	BRC	49.01	0.270	0.977	19.96	4.84	0.930	48.43	0.00118	0.954
	BDC	95.50	2.122	0.976	55.05	6.85	0.899	96.75	0.00026	0.948
MG	SRC	156.43	0.105	0.948	36.41	3.303	0.847	148.89	0.00234	0.961
	SDC	176.37	0.139	0.940	45.05	3.459	0.825	169.68	0.00183	0.954
	BRC	86.55	0.385	0.981	33.85	4.511	0.901	84.07	0.00072	0.976
	BDC	109.82	0.649	0.978	43.10	4.218	0.889	106.87	0.00045	0.973
MO	SRC	82.05	0.0038	0.853	0.29	1.036	0.946	63.87	0.03391	0.977
	SDC	93.49	0.0033	0.860	0.27	0.958	0.932	88.70	0.0354	0.970
	BRC	133.29	0.0017	0.774	0.11	0.872	0.940	65.90	0.04114	0.981
	BDC	181.28	0.0012	0.746	0.09	0.842	0.923	74.43	0.04441	0.965

The adsorption isotherm forms of methyl orange are type S in Giles classification. The S-curve is generally result of “cooperative adsorption”, with solute molecules tending to be adsorbed packed in rows or clusters [31]. A type S isotherm appears when the binding energy of the first layer is lower than the binding energy between water molecules. This is due to the fact that methyl orange is an anionic molecule that has the same charge of clays surface. Consequently, low adsorption affinity is observed. A physisorption assured by Van der Waals interactions is suggested. The best fit of experimental data was obtained by the Dubinin–Radushkevich isotherm model with maximum adsorption capacities of 63.87, 88.70, 65.90 and 74.43 mg/g, respectively, for SRC, SDC, BRC and BDC.

From these results, it was clear that the adsorption of methylene blue and malachite green is more correlated to cationic exchange capacity and BET surface area than that of methyl orange.

3.5. Effect of temperature

Evaluation of temperature was carried out with the scope of testing the ability of the clays in dyes removal in the case of different kinds of effluents, bearing in mind the specific circumstances of dyestuff wastes. Data were collected at five temperatures from 10 to 50 °C. The quantities of MB, MG and MO adsorbed on the clays as function of solution temperature are shown in Table 5. The table indicates that the increase in solution temperature increases the adsorbed quantities of MG. However,

Table 5

Thermodynamic parameters calculated for the adsorption of dyes by the clays.

Clay	T (°C)	MB					MG					MO				
		q_e (mg/g)	K_D	ΔG° (J/mol)	ΔH° (kJ/mol)	ΔS° (J/K mol)	q_e (mg/g)	K_D	ΔG° (J/mol)	ΔH° (kJ/mol)	ΔS° (J/K mol)	q_e (mg/g)	K_D	ΔG° (J/mol)	ΔH° (kJ/mol)	ΔS° (J/K mol)
SRC	10	72.7	2.67	-2311.5	-13.6	-40.3	156.6	7.24	-1607.5	45.2	175.5	64.7	1.83	-1424.1	-33.9	-112.9
	20	66.6	2.00	-1691.1			169.8	11.32	-2159.2			62.7	1.68	-1265.6		
	30	61.6	1.61	-1198.6			183.7	23.04	-2880.2			50.3	1.01	-35.2		
	40	58.1	1.39	-865.8			191.8	47.31	-3512.6			37.2	0.59	1364.9		
	50	56.8	1.32	-748.3			194.4	69.39	-3879.1			24.6	0.33	3008.9		
SDC	10	80.3	4.10	-3321.9	-10.5	-25.2	165.1	9.52	-1911.5	49.1	190.8	63.5	1.74	-1304.9	-36.3	-121.0
	20	78.7	3.72	-3201.7			175.2	14.21	-2377.6			64.9	1.85	-1499.3		
	30	76.1	3.20	-2929.6			187.2	29.26	-3065.2			49.5	0.98	46.9		
	40	743	2.90	-2768.2			194.4	69.39	-3759.1			39.2	0.64	1146.4		
	50	69.8	2.32	-2256.9			196.4	109.25	-4152.1			20.9	0.26	3580.2		
BRC	10	46.5	0.87	318.90	-7.5	-27.4	107.0	2.31	415.1	14.7	58.8	57.2	1.34	-686.9	-10.0	-32.4
	20	43.9	0.78	590.14			107.8	2.35	381.2			55.4	1.24	-527.9		
	30	41.5	0.71	855.24			132.5	3.95	-799.1			55.5	1.25	-558.1		
	40	41.8	0.72	855.15			140.8	4.78	-1163.4			57.2	1.34	-753.3		
	50	37.0	0.59	1418.07			135.7	4.24	-989.6			43.9	0.78	654.7		
BDC	10	94.6	17.69	-6760.5	-3.8	10.2	127.5	3.53	-548.4	42.8	160.3	42.3	0.73	734.04	-26.6	-94.6
	20	94.6	17.69	-6999.2			143.9	5.16	-1207.4			41.1	0.70	879.63		
	30	93.7	14.84	-6794.9			164.3	9.25	-2013.9			37.2	0.59	1313.84		
	40	93.6	14.70	-6994.3			166.8	10.10	-2181.8			23.3	0.30	3103.27		
	50	93.5	14.56	-7192.2			191.2	43.55	-3566.5			15.9	0.19	4477.28		

the adsorbed quantity of MO decreases significantly with the increase in temperature. The adsorption of MB is less influenced by the temperature, the adsorbed amounts slightly decreases with the increase of solution temperature from 10 °C to 50 °C. From these results, thermodynamic parameters including the change in free energy (ΔG°), enthalpy (ΔH°) and entropy (ΔS°) were used to describe thermodynamic behavior of the adsorption of MB, MG and MO onto the clays. These parameters were calculated by considering the following reversible process [32]:



For such equilibrium reactions, K_D , the distribution constant, can be expressed as:

$$K_D = \frac{q_e}{C_e} \quad (13)$$

The Gibbs free energy is:

$$\Delta G^\circ = -RT \ln(K_D) \quad (14)$$

where R is the universal gas constant (8.314 J mol/K) and T is solution temperature in K.

The enthalpy (ΔH°) and entropy (ΔS°) of adsorption were estimated from the slope and intercept of the plot of $\ln K_D$ versus $1/T$ yields, respectively.

$$\ln K_D = -\frac{\Delta G^\circ}{RT} = -\frac{\Delta H^\circ}{RT} + \frac{\Delta S^\circ}{R} \quad (15)$$

The calculated constants are also illustrated in Table 5. From the table, it can be concluded that, the adsorption process was found to be exothermic in nature in the case of MB and MO. Also, the magnitude of enthalpies gives information on the type of adsorption, which can be either physical or chemical. The reaction was accompanied by a decrease in entropy. The negative ΔS° value suggests a decrease in the randomness at the solid/solution interface during the adsorption. The Gibbs energy (ΔG°) increased when the temperature was increased from 10 to 50 °C indicating a decrease in feasibility of adsorption at higher temperatures. In the case of MG, the adsorption was endothermic and accompanied by a decrease in ΔG° values with the increase in temperature. This result indicates an increase in feasibility of adsorption at higher temperatures. The ΔS° values were found to be positive which suggests an increase in the randomness at the solid/solution interface during the adsorption. From all this results, it could be concluded that adsorption of methyl orange was more influenced by the change in solution temperature.

4. Conclusions

This study shows that Moroccan natural clays can efficiently remove dyes from aqueous solutions. The adsorption was dependent on the pH of the aqueous solution, with a high uptake of cationic dyes at high pH, and high uptake of anionic dye at low pH. The adsorption was rapid and could be considered to fit pseudo-second order kinetics model in the case of methylene blue and malachite green. The equilibrium uptake was increased with increasing the initial concentration of dye in solution. The adsorption isotherm could be well fitted by Langmuir equation in the case of cationic dyes and Dubinin–Radushkevich equation in the case of anionic dye. The adsorption capacity of cationic dyes was found to be higher than anionic dye. The rise in temperature increases the adsorbed amount of malachite green and decreases the adsorbed amount of methyl orange and methylene blue dyes. The adsorption of cationic dyes is more correlated to cationic exchange capacity and BET surface area than that of anionic dye. The adsorption of anionic dye was more influenced by the change in solution temperature. These results suggest that the adsorption of cationic dyes by the clays could be chemisorption. However, a physisorption is proposed for the adsorption of anionic. Finally, the use of Moroccan natural clays shows a greater potential for the removal of textile dyes, as no costly equipment is required.

References

- [1] H. Zollinger, *Color Chemistry: Synthesis, Properties and Applications of Organic Dyes and Pigments*, VCH, New York, NY, 1991.
- [2] A. Reife, *Dyes environmental chemistry*, in: *Kirk-Othmer Encyclopedia of Chemical Technology*, John-Wiley & Sons New York, NY, 1993.
- [3] N. Barka, A. Assabbane, Y. Aït Ichou, A. Nounah, Decantation of textile wastewater by powdered activated carbon, *J. Appl. Sci.* 6 (3) (2006) 692–695.
- [4] M.A. Ahmad, N.A. Ahmad Puad, O.S. Bello, Kinetic, equilibrium and thermodynamic studies of synthetic dye removal using pomegranate peel activated carbon prepared by microwave-induced KOH activation, *Water Resour. Ind.* 6 (2014) 18–35. <http://dx.doi.org/10.1016/j.wri.2014.06.002>.
- [5] M. Dogan, H. Abak, M. Alkan, Adsorption of methylene blue onto hazelnut shell: kinetics, mechanism and activation parameters, *J. Hazard. Mater.* 164 (2009) 172–181.
- [6] A. Gurses, A. Hassani, M. Kiransan, O. Acisli, S. Karaca, Removal of methylene blue from aqueous solution using by untreated lignite as potential low-cost adsorbent: kinetic, thermodynamic and equilibrium approach, *J. Water Process Eng.* (2014). <http://dx.doi.org/10.1016/j.jwpe.2014.03.002>.
- [7] N. Barka, A. Assabbane, A. Nounah, L. Laanab, Y. Aït Ichou, Removal textile dyes from aqueous solution by Natural Phosphate as new adsorbent, *Desalination* 235 (2009) 264–275.
- [8] F.C. Tsai, N. Ma, T.C. Chiang, L.C. Tsai, J.J. Shi, Y. Xia, T. Jiang, S.K. Su, F.S. Chuang, Adsorptive removal of methyl orange from aqueous solution with crosslinking chitosan microspheres, *J. Water Process Eng.* 1 (2014) 2–7.
- [9] M. Zarezadeh-Mehrzi, A. Badiei, Highly efficient removal of basic blue 41 with nanoporous silica, *Water Resour. Ind.* 5 (2014) 49–57.
- [10] M. Dogan, M.H. Karaoglu, M. Alkan, Adsorption kinetics of maxilon yellow 4GL and maxilon red GRL dyes on kaolinite, *J. Hazard. Mater.* 165 (2009) 1142–1151.
- [11] N. Barka, S. Qourzal, A. Assabbane, A. Nounah, Y. Ait-Ichou, Removal of reactive yellow 84 from aqueous solutions by adsorption onto hydroxyapatite, *J. Saudi Chem. Soc.* 15 (2011) 263–267.
- [12] N. Barka, S. Qourzal, A. Assabbane, A. Nounah, Y. Aït-Ichou, Adsorption of Disperse Blue SBL dye by synthesized poorly crystalline hydroxyapatite, *J. Environ. Sci.* 20 (2008) 1268–1272.
- [13] M. Dogan, M. Alkan, Adsorption kinetics of methyl violet onto perlite, *Chemosphere* 50 (2003) 517–528.
- [14] Y. Ozdemir, M. Dogan, M. Alkan, Adsorption of cationic dyes from aqueous solutions by sepiolite, *Microporous Mesoporous Mater.* (2006) 419–427.
- [15] A.H. Gemeay, A.S. El-Sherbiny, A.B. Zaki, Adsorption and kinetic studies of the intercalation of some organic compounds onto Na⁺-montmorillonite, *J. Colloid Interface Sci.* 245 (2002) 116–125.
- [16] N. Barka, K. Ouzaouit, M. Abdennouri, M. El Makhfouk, Dried prickly pear cactus (*Opuntia ficus indica*) cladodes as a low-cost and eco-friendly biosorbent for dyes removal from aqueous solutions, *J. Taiwan Inst. Chem. Eng.* 44 (2013) 52–60.
- [17] N. Barka, M. Abdennouri, M.E.L. Makhfouk, Removal of Methylene Blue and Eriochrome Black T from aqueous solutions by biosorption on *Scolymus hispanicus* L.: kinetics, equilibrium and thermodynamics, *J. Taiwan Inst. Chem. Eng.* 42 (2011) 320–326.
- [18] W.T. Tsai, C.Y. Chang, C.H. Ing, C.F. Chang, Adsorption of acid dyes from aqueous solution on activated bleaching earth, *J. Colloid Interface Sci.* 275 (2004) 72–78.
- [19] Z. Boubberka, A. Khenifi, N. Benderdouche, Z. Derriche, Removal of Supranol Yellow 4 GL by adsorption onto Cr-intercalated montmorillonite, *J. Hazard. Mater.* 133 (2006). 154–151.
- [20] S. Yariv, H. Cross, *Organo-clay Complexes and Interaction*, Marcel Dekker, New York, NY, 2001.
- [21] M. Abdennouri, M. Baalala, A. Galadi, M. El Makhfouk, M. Bensitel, K. Nohair, M. Sadiq, A. Boussaoud, N. Barka, Photocatalytic degradation of pesticides by titanium dioxide and titanium pillared purified clays, *Arabian J. Chem.* (2011) <http://dx.doi.org/10.1016/j.arabjch.2011.04.005>.
- [22] I. Langmuir, The constitution and fundamental properties of solids and liquids, *J. Am. Chem. Soc.* 38 (1916) 2221–2295.
- [23] H. Freundlich, W. Heller, The adsorption of cis- and trans-azobenzene, *J. Am. Chem. Soc.* 61 (1939) 2228–2230.
- [24] M.M. Dubinin, L.V. Radushkevich, The equation of the characteristic curve of the activated charcoal, *Proc. Acad. Sci. USSR Phys. Chem. Sec* 55 (1947) 331–337.
- [25] B.H. Hameed, A.A. Ahmad, N. Aziz, Adsorption of reactive dye on palm-oil industry waste: equilibrium, kinetic and thermodynamic studies, *Desalination* 247 (2009) 551–560.
- [26] S. Lagergren, About the theories of so-called adsorption of soluble substance *Seven Vetenskapsakad, Handband* 24 (1898) 1–39.
- [27] Y.S. Ho, G. McKay, The kinetics of sorption of basic dyes from aqueous solution by sphagnum mass peat, *Can. J. Chem. Eng.* 76 (1998) 822–827.
- [28] W.J. Weber Jr., J.C. Morris, Kinetics of adsorption on carbon from solution, *J. Sanitary Eng. Div. ASCE* 89 (1963) 31–59.
- [29] Y.S. Ho, G. McKay, Pseudo-second-order model for sorption processes, *Process Biochem.* 34 (1999) 451–465.
- [30] C.H. Giles, T.H. MacEvan, S.N. Nakhwa, D. Smith, Studies on adsorption-XI, *J. Chem. Soc.* 111 (1960) 3973–3993.
- [31] C.H. Giles, A.P. D'Silva, I.A. Easton, A general treatment and classification of the solute adsorption isotherm. II. Experimental interpretation, *J. Colloid Interface Sci.* 47 (3) (1974) 766–778.
- [32] I. Bakas, K. Elatmani, S. Qourzal, N. Barka, A. Assabbane, I. Aït-Ichou, A comparative adsorption for the removal of p-cresol from aqueous solution onto granular activated charcoal and granular activated alumina, *J. Mater. Environ. Sci.* 5 (3) (2014) 675–682.